We are IntechOpen, the world's leading publisher of Open Access books Built by scientists, for scientists

6,900
Open access books available

185,000
International authors and editors

200M
Downloads

Our authors are among the

154
Countries delivered to

TOP 1%
most cited scientists

12.2%
Contributors from top 500 universities



WEB OF SCIENCE™

Selection of our books indexed in the Book Citation Index in Web of Science™ Core Collection (BKCI)

Interested in publishing with us?
Contact book.department@intechopen.com

Numbers displayed above are based on latest data collected.
For more information visit www.intechopen.com



8

Fast Method for Frequency Measurement by Rational Approximations with Application in Mechatronics

Daniel Hernandez-Balbuena[1], Oleg Sergiyenko[2],
Patricia L. A. Rosas-Méndez[1], Vera Tyrsa[3] and Moises Rivas-Lopez[2]
[1]*Engineering Faculty, Autonomous University of Baja California*
[2]*Engineering Institute of Autonomous University of Baja California*
[3]*Polytechnic University of Baja California, Mexicali*
México

1. Introduction

In Automatic Control, Mechatronics and Robotics technical tasks is desirable to have information about certain parameters to control, supervision or fault detection in a system. This information can be estimates by direct measurement of particular variables or using special devices capable of observing the state of system under control. If the first option is selected a physical sensor is required.

One commonly selected option are the Frequency Domain Sensors (FDS), this devices converts the desired parameter into a square wave with a frequency or period proportional to physical quantity under measurement. In order to reduce time to obtain information for control a system with sufficient quality and good reliability, a high performance method for frequency measurement is desirable.

Historically, many analog and digital frequency measurement techniques have been proposed. In a basic digital measurement technique, the zero crossings of a signal are detected and a square wave is formed, representing transitions between the binary logic levels low and high. Selected digital logic state is detected and counted, and a measure of frequency is determined by the number of complete cycles occurring in the square waveform during a fixed time interval, determined by the counter's time base [1]. This method can be classified as the classical method and their main error source is the ± 1 error count derived from the relative timing of gate and signal, which means that the resolution is 1 Hz during a 1s gate time for all input signal frequencies [2]. For allow high resolution frequency measurements gate time larger than 1s should be selected.

In reciprocal counting measurement techniques, the gate time is determined by electronic detection of two kinds of same phase difference situations between two pulsed signals with

different frequencies [3], or by electronic detection of two coincident pulses of two regular independent pulse trains [5 -6]. In these methods the quantization error (±1 count error) can be overcome satisfactorily [2-3,6]. But, in [3] a high distinguishability analog circuit for phase coincidence detection is required and in [5] the relative methodical error is pulse width dependent for random selection of stop measurement pulse coincidence and, is experimentally probed that relative methodical error can be reduced by two o three orders of magnitude than frequency meters based on classical method [6].

Continuous time stamping principle change the scenario in frequency measurement, because in each measurement has not a defined start (= start trigger event), and a stop (= stop trigger event) plus a dead-time between measurements to read out and clear registers, do interpolation measurements and prepare for next measurement [2]. In this technique Linear regression using the least-squares line fitting is used because for a one-second frequency measurement in a fast processing counter could contain hundreds o thousands of paced time-stamped events, no just a start event plus a stop event [2]. But fast digital circuits are needed to implement this technique.

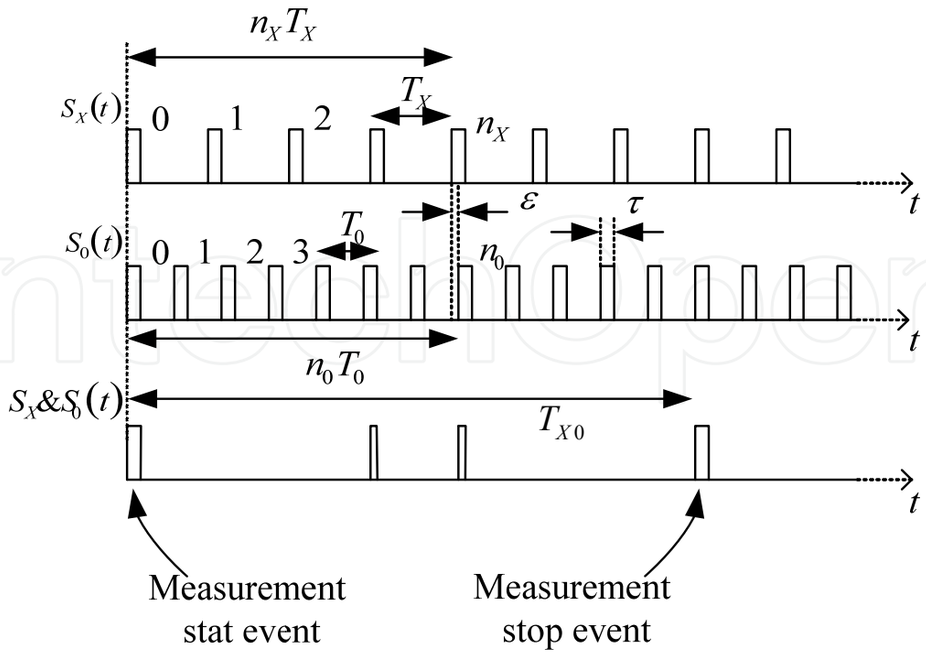
However, a fast method for frequency measurement base pulse coincidence principle and rational approximations was proposed and, was shown that under a novel numerical condition for detect the stop trigger event measurement resolution is improved. Instrumental errors are caused only by the reproducibility of the reference frequency and relative measurement error is comparable to the reproducibility of reference oscillator. [7]. Simple digital circuits are needed to practical implementation of this technique.

2. Frequency measurement based on the pulse coincidence principle

In the past, pulse coincidence principle has been used for frequency measurement of electrical signals [4-6]. In this measurement method, a desired frequency is measured by comparing it with a standard frequency. The zero crossings of both frequencies are detected, and a narrow pulse is generated at each crossing. Then, two regular independent pulse trains are generated. The desired and standard trains of narrow pulses are compared for coincidence. This is made with an AND-gate, and then a coincidence pulse train is generated. Coincident pulses can be used as triggers to start and stop a pair of digital counters (start and stop events). See Figure 1.

The standard and desired pulse trains are applied to other counters and a measure of the desired frequency is obtained by multiplying the known standard frequency by the ratio between the desired count and the standard count obtained in the two digital counters [5]. And basically, measurement error reduction depends on the ability to detect a pair of *best* coincidences consecutively between a large number of these, for a given measurement time. In other works, measurement error reduction depends on reduction of comparison error of time intervals n_0T_0 and n_XT_X by selection of adequate coincidence pulses [6].

Consider f_x as the desired or unknown frequency and f_o as the standard frequency, and $T_x = 1/f_x$ and $T_o = 1/f_o$ are they periods respectively. In Figure 1, $S_X(t)$ and $S_0(t)$ are the unknown and standard trains of narrows pulses, τ is the pulse width on both trains and, $S_X(t)$ &$S_0(t)$ is the irregular pulse coincidence train. Then, n_0 and n_X are integer numbers and represent the amount of whole periods between selected measurement start and stop events (see figure 1).



a)

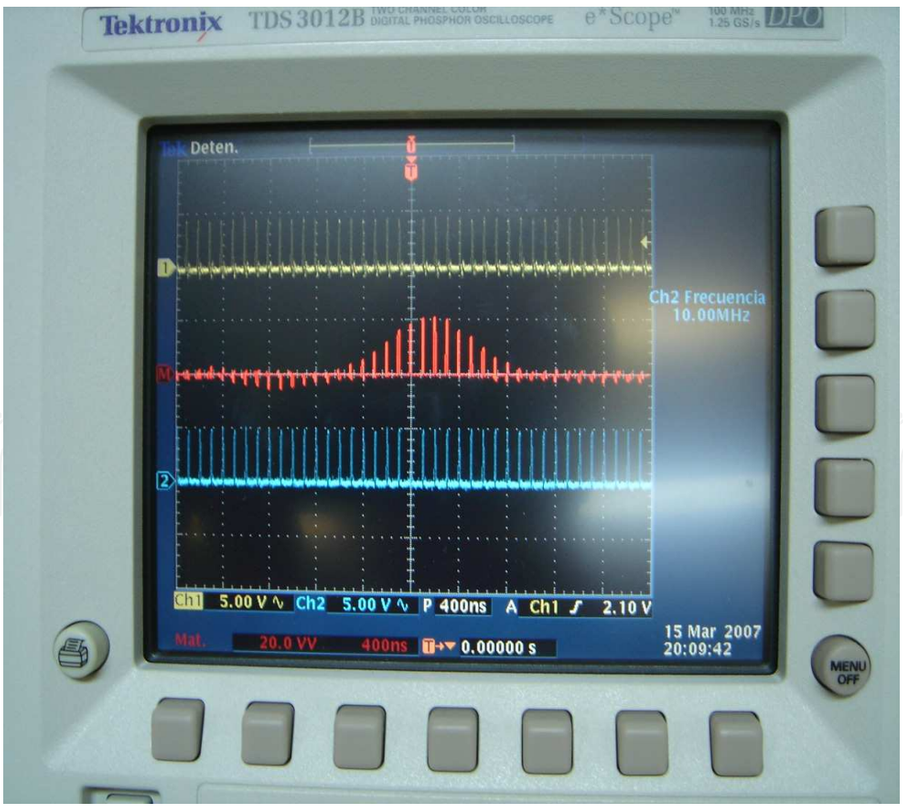


Fig. 1. a) Pulse coincidence principle for frequency measurement, b) Practical view of coincidences process (oscilloscope screenshot).

In [6] by possible selection of *partial* coincidences, error of comparison of time intervals n_0T_0 and n_XT_X has been reduced to the duration of the coinciding pulses and mathematically expressed by

$$\left|n_XT_X - n_0T_0\right| \le 2\tau. \tag{1}$$

Form (1), relative measurement error for a single measurement can be expressed as follows

$$\beta_X = \frac{\left|f_X - \frac{n_X}{n_0}f_0\right|}{f_X} \le \frac{2\tau}{n_0T_0} \approx \frac{2\tau}{t_m}, \tag{2}$$

where t_m is the measurement time.

It is experimentally known, that for a standard frequency $f_0 = 1\times10^6$ Hz from a thermostatic quartz generator with relative short-term instability does not exceed 10^{-8} and using a pulses width $\tau \approx 7\times10^{-9}$ s, root-mean-square (RMS) error $s_X = 14.3\times10^{-6}$ Hz for $f_X = 1\times10^3$ Hz at 50 observations during total measurement time $t_m \le 1$ s. And $s_x = 1.79\times10^{-3}$ Hz for $f_X = 1\times10^6$ Hz under same measurement conditions [6].

2.1 functioning and uncertainty limitations

Let us consider two trains of narrow pulses with period T_X and T_0 with and pulse width τ respectively, generated by detection of zero crossings of two sinusoidal signal of frequencies f_0 and f_X. Suppose that T_0 is a known parameter and T_X is unknown and, both pulse trains start in phase, i.e. a time shift is 0.

For an appropriate selection of the pulse width of two regular independent pulse trains, periodic perfect coincidences of these pulses are observed in time axis [13]. Repetition period of perfect coincidences is T_{X0}, in Fig. 1a). A Practical view of coincidences process is presented in Fig 1 b).

For frequency measurement, the time intervals n_0T_0 and n_XT_X are compared, where n_0 is the amount of periods T_0 in the measurement time and n_X is the amount of periods T_X in the same time interval.

Measurement time can be defined by the time interval between the first one pulse of coincidence (start event) after beginning the measurement process, and by any other following pulse of coincidence (stop event). As it were mentioned in the previous section, n_0 and n_X are the counts of pulses obtained in two digital counters.

According to [12], pulse coincidence occurs when

$$\left|n_XT_X - n_0T_0\right| \le \varepsilon \tag{3}$$

where ε is the acceptable tolerance (reasonable error value between time intervals n_0T_0 and n_XT_X less to pulse with and dependent on the quality of electronic circuits used).

To find values of n_0 and n_X which define the appropriated coincidence it is useful to expand T_X/T_0 as simple continued fractions. This is evident rewriting (3)

$$\left|\frac{T_X}{T_0}-\frac{n_0}{n_X}\right|\le\frac{\varepsilon}{n_X T_0}. \tag{4}$$

Left side of equation (3) represents the approximation of T_X/T_0 using rational numbers and right side is an approximation condition.

For frequency measurement, in a view of $f_0=1/T_0$, $f_X=1/T_X$, we can write

$$\left|f_X-\frac{n_0}{n_X}f_0\right|\le\frac{\varepsilon f_X f_0}{n_0}. \tag{5}$$

In (5), f_X is the hypothetical true value of the unknown frequency and $f_0 n_0/n_X$ is the frequency value obtained by the measurement. Then, dividing both parts of (5) in f_X and taking to account $f_0=1/T_0$, relative error of measurement (frequency offset) β can been expressed by

$$\beta=\left|f_X-\frac{n_0}{n_X}\right|\Big/f_X\le\frac{\varepsilon}{n_0 T_0}. \tag{6}$$

We can see in equation (6) that relative error of measurement is limited by the ratio between the acceptable tolerance of the error of comparison between the time intervals n_0T_0 and n_XT_X and, the time interval n_0T_0 . Value of n_0T_0 is approximately the measurement time.

2.2 Numerical stop condition of measurement

In frequency measurement, n_0 and n_X are independent counter counts obtained in two digital counters, so they are properly integer numbers. An integer numbers ratio, like the involved in the frequency value obtained by the measurement, is possible to investigate under number theory laws. Let note and briefly explain some of them, especially Euclidean algorithm.

2.2.1 Number theoretic preliminaries

Let us to assume without loss generality that $T_X>T_0$, from the division algorithm we can write

$$T_X=a_0T_0+\Delta t_0 \quad T_0>\Delta t_0\ge 0 \tag{7}$$

$$T_0=a_1\Delta t_0+\Delta t_1 \quad \Delta t_0>\Delta t_1\ge 0 \tag{8}$$

$$\Delta t_0=a_2\Delta t_1+\Delta t_2 \quad \Delta t_1>\Delta t_2\ge 0 \tag{9}$$

$$\vdots \qquad\qquad \vdots$$

$$\Delta t_{i-2} = a_i \Delta t_{i-1} + \Delta t_i \quad \Delta t_{i-1} > \Delta t_i \geq 0 \tag{10}$$

$$\vdots \qquad\qquad \vdots$$

$$\Delta t_{n-2} = a_n \Delta t_{n-1} + \Delta t_n \quad \Delta t_{n-1} > \Delta t_n \geq 0 \tag{11}$$

where the a_i is the *i*th partial quotients for each case and Δt_i is the *i*th remainder, with $i = 1,2,3,...,n$. With $a_i \geq 1$, Δt_i is a decreasing sequence for $i \geq 0$.

Each remained obtained in the division step of Euclidean algorithm be could be interpreted as a distance [11], defined by

$$\left| Q_i T_X - P_i T \right|_0 = \Delta t_i. \tag{12}$$

where P_i and Q_i are the numerator and denominator of the *i*th convergent of the continued fractions to T_X / T_0 defined recursively as [12]

$$P_i = a_i P_{i-1} + P_{i-2} \tag{13}$$

$$Q_i = a_i Q_{i-1} + Q_{i-2} \tag{14}$$

for arbitrary $i \geq 2$, and

$$P_0 = a_0, \qquad Q_0 = 1,$$
$$P_1 = a_0 a_1 + 1, \quad Q_1 = a_1.$$

Then, from (12) each remainder Δt_i is the absolute difference between the time intervals $Q_i T_X$ and $P_i T_0$.

On the other hand, T_0 can be expressed in terms of two consecutive remainders [11] using the following expression:

$$T_0 = Q_i \Delta t_{i-1} + Q_{i-1} \Delta t_i \,. \tag{15}$$

A similar expression can be derived for T_X

$$T_X = P_i \Delta t_{i-1} + P_{i-1} \Delta t_i \,. \tag{16}$$

Supposing that n is the number of steps in the Euclidean algorithm to obtain greatest common divisor of T_X and T_0. Then last remained $\Delta t_n = 0$ and time interval Δt_{n-1} is the greatest common divisor of both periods T_X and T_0, in the consecutive division expressed in equations (7) to (11). Because the greatest common divisor is: the last nonzero remainder in this sequence of divisions.

Assuming that Δt_{n-1} is greatest common divisor of both periods T_X and T_0, we can write

$$T_0 = Q_n \Delta t_{n-1} \tag{17}$$

$$T_X = P_n \Delta t_{n-1} \,. \tag{18}$$

Expressing (10) in terms of (15) and (16) it is evident in (17) than step n is total equality point for both time intervals

$$\left|Q_n P_n \Delta t_{n-1} - P_n Q_n \Delta t_{n-1}\right| = 0. \tag{19}$$

In frequency measurement, this term expressed in several forms have a mathematical mean of least common multiple, and practical mean of time interval T_{X0} (see Fig. 1) expressed by:

$$T_{XO} = \frac{T_X T_0}{\Delta t_{n-1}} = P_n Q_n \Delta t_{n-1} \tag{20}$$

is the condition for periodic perfect coincidences of pulses (see Fig. 1). Assuming to T_{X0} the measurement time in frequency measurement, from (1) and Fig. 1

$$\left|n_X T_X - n_0 T_0\right| = 0 \cdot \tag{21}$$

and each time intervals $n_0 T_0$ and $n_X T_X$ are equal to T_{X0}. Then,

$$n_0 T_0 = P_n Q_n \Delta t_{n-1}, \tag{22}$$

$$n_X T_X = P_n Q_n \Delta t_{n-1} \cdot \tag{23}$$

Now, product of two numbers $ab = c$ can be considered as the sum $a + a + a + \cdots + a$ in which the number of summands is equal to b or as the sum $b + b + b + \cdots + b$ in which the number of summands is equal to a.

Then, equations (22) and (23) can be rewrited using (17) and (18):

$$n_0 Q_n \Delta t_{n-1} = P_n Q_n \Delta t_{n-1},$$

$$n_X P_n \Delta t_{n-1} = P_n Q_n \Delta t_{n-1} \cdot$$

Expressions (22) and (23) have a reason only when

$$n_0 = P_n \tag{24}$$

and

$$n_X = Q_n. \tag{25}$$

2.2.2 Stop condition of measurement

For small measurement time (less than or equal a 1 s) is evident from equation (4) that: order of magnitude of Δt_{n-1} must be of same order of magnitude that the expected relative error of measurement β. Then, according to before mentioned, we propose that an acceptable tolerance in (1) is $\varepsilon = \Delta t_{n-1}$.

Assuming decimal notation for both periods T_X and T_0, under the conditions $T_X < 1$ and $T_0 < 1$, and assuming reference period can be expressed as $T_0 = 1 \times 10^{-s}$, then the greatest common divisor Δt_{n-1} is

$$\Delta t_{n-1} = \left(T_X, T_0\right) = \frac{1}{10^r}\left(A, 10^{r-s}\right) \tag{26}$$

where A, r, s are integer numbers with $r > s$, r is the exponent associate to expected the order of magnitude of β, $r-s$ is the difference between the expected order of magnitude β and the order of magnitude of the time period of the standard.

On the other hand, according with equation (25) the number of time intervals T_X necessaries to stop the measurement process is Q_n, and form (15)

$$Q_n = \frac{T_0}{\Delta t_{n-1}}. \tag{27}$$

If A and 10^{r-s} in equation (26) are mutually prime then $\Delta t_{n-1} = 10^{r-s}$ and

$$Q_n = 10^{r-s} \tag{28}$$

and, if they are not, then $\Delta t_{n-1} = a/10^r$ whit a integer number and

$$Q_n = 10^{r-s} / a. \tag{29}$$

In both cases $1/10^r$ is a common divisor of both periods T_X and T_0.

Then, from equations (16), (24) and (25), the condition that satisfies (19) is

$$n_X = 10^{r-s}. \tag{30}$$

This is the numeric condition that we propose to stop the measurement process and is easy to implement with basics digital circuits.

A novel fast method to frequency measurement with application in mechatronics and telecommunication is based on this numerical stop condition is presented in [7-9]. Resolution improvement in frequency domain sensors is allowed in automotive applications [10] with this method and is applied in precise optical scanning and structural health monitoring [19-21]

3. Simulation

In the simulation two pulse trains of unitary amplitude are generated using a computational algorithm sampling independent [7]. The value of reference frequency was accepted as $f_0 = 1\times10^7$ Hz. The hypothetical value of unknown frequency is $f_X = 5878815.277629991$ Hz, and is a result of the accepted value of the period $T_X = 1.701023\times10^{-7}$ s. The value of pulse width in both pulse trains is accepted as $\tau = 1.5\times10^{-9}$ s.

In this case, is evident that T_X and T_0 are mutually prime numbers and have the common denominator $\Delta t_{n-1} = 1\times10^{-13}$.

Simulation algorithm provided continuous formation of the segments n_0T_0 and n_XT_X and compares the magnitude of their difference with parameter 2τ. When the value of the

specified difference was less than 2τ on corresponding steps of simulation, it was identified like a coincidence of pulses and the integer numbers n_0 and n_X are stored.

The unknown frequency is calculated using $f_{Xm} = n_x f_0 / n_0$ and frequency relative error is obtained using $(f_X - f_{Xm})/fx$, both results are stored also.

Simulation results are partially presented in the Table 1 and, frequency relative error calculated (non absolute value) is presented in Fig. 2 for a simulation time of 0.2 s.

The simulation process star in $n_0 = 0$ and $n_X = 0$, and the best approximation is selected (in this case) using the condition, $n_X = 1 \times 10^6$.

Table 1 represents an interesting fact. For thousands of data we have the same uncertainty range 10^{-13}, as for first and third rows. And only when n_X takes a form of 1 with six zeros (in this case, second row of Table 1) we are getting up to 10^{-17}.

In Fig. 2, we can see a global convergence to zero of frequency relative error. An alternated convergence and a non monotone decreasing characteristic are evident. However, we can identify in the graphic a point where β is minimum for an approximated time of 0.17 s.

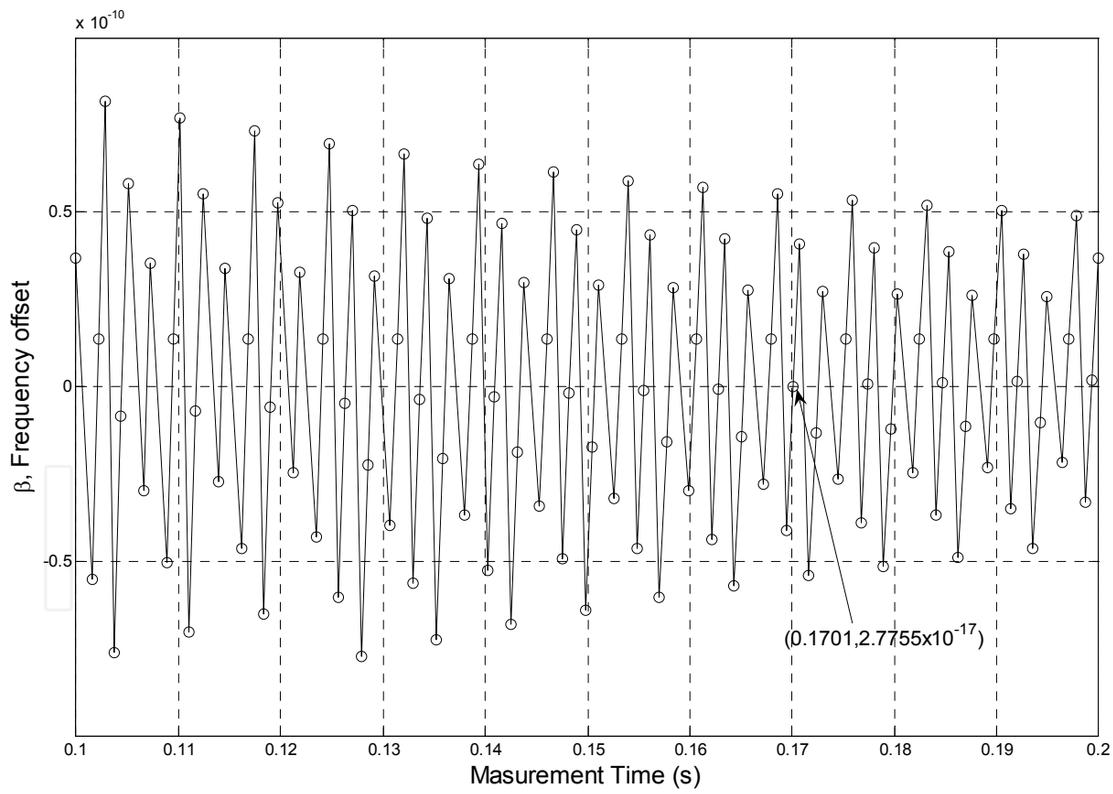


Fig. 2. Frequency offset from the simulation process

Frequency offset from computational selection of best coincidences, obtained under condition (1) with $\varepsilon = 1 \times 10^{-12}$ is presented in Fig. 3. In this graphic, we can observe a convergence by the left and a divergence by the right around 0.17 s (first point in the Fig. 3).

This condition is repeated with time, and we can see five points where absolute value of β is minimum, for a simulation time of 1 s. In each mentioned points the condition expressed in (30) is fulfilled.

n_X	n_0	$\lvert n_X T_X - n_0 T_0 \rvert$,s	f_{Xm} , Hz
957087	1628027	1.00×10^{-13}	5878815.277633602
1000000	1701023	2.78×10^{-17}	5878815.277629991
1042913	1774019	1.00×10^{-13}	5878815.277626677

Table 1. Simulation results of frequency measurement process.

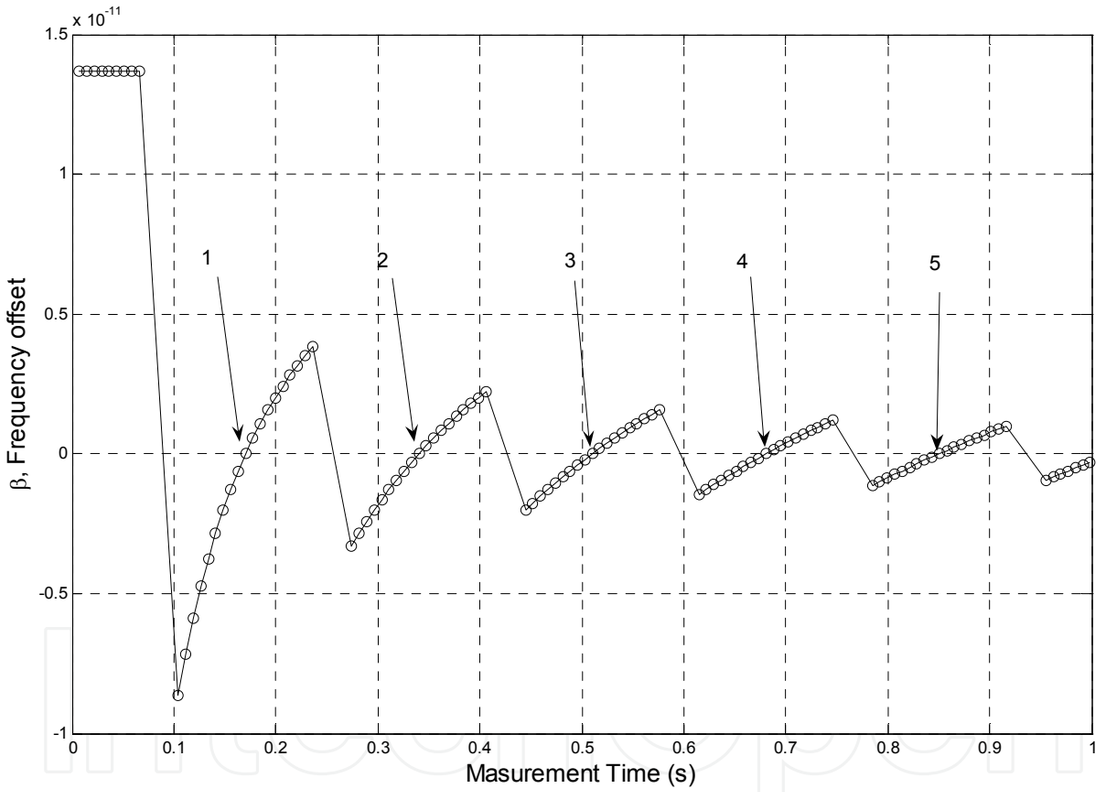


Fig. 3. Frequency offset from the simulation process for 1 s.

3.1 Jitter effect in frequency measurement

In order to evaluated the jitter effect on the non-electrically detectable stop event for frequency measurement method based on the direct comparison of two regular independent trains of narrow pulses and rational approximations. Deterministic and random components of jitter are modeled and, are added in both pulse trains one deterministic jitter component and random jitter in each case. Simulation results are presented when both pulse trains start in phase and when start with a phase shift.

Timing jitter (henceforth referred to as jitter) is defined as short-term non-cumulative variations of the significant instants of a signal from their ideal positions in time [18].

For modeling, Total Jitter (TJ) consists of two components: Deterministic Jitter (DJ) and Random Jitter (RJ) [14]. In time domain, TJ is the sum of the RJ and DJ components [15]. RJ is characterized by a Gaussian distribution. It has been shown that it is theoretically unbounded in amplitude.

DJ consists of several components caused by different and mostly physically-based phenomena, such electronic interference, cross-talk and bandwidth limitation. All DJ subcomponents have a bounded peak-to-peak value that does not increase when more measurement samples are taken [15].

Deterministic jitter has four components: duty cycle distortion (DCD), intersymbol interference (ISI), periodic jitter (PJ) and bounded uncorrelated jitter (BUJ).

DCD and ISI are referred as data correlated jitter, while PJ and BUJ are referred as data uncorrelated jitter. RJ is unbounded and uncorrelated [15].

3.1.1 Random Jitter (RJ)

Random Jitter RJ is caused the common influence of a large number of very small independent contributor or various device-originated noise sources (such as thermal and flicker noise). By the central limit theorem, the distribution of a large number of uncorrelated noise sources approaches a probability Gaussian distribution and is given by [14]

$$J_{RJ}(x) = \frac{1}{\sigma\sqrt{2\pi}} e^{-\left(\frac{x^2}{2\sigma^2}\right)} \tag{31}$$

where σ is the standard deviation of the jitter distribution or the RMS value, and J_{RJ} is the probability that leading edge (or trailing edge) will occur at time x, where x is the deviation from the mean value of the time reference point (time point related to 50% amplitude point on pulse edge). In Fig. 4a), is shows the histogram for random jitter.

3.1.2 Periodic Jitter (PJ)

Periodic jitter denotes periodical timing deviation from the ideal position of a signal that repeat in time, is typically uncorrelated to the data rate or the clock frequency [14]. Electromagnetic interference and crosstalk from some clock line can cause periodic jitter.

The mathematic model of PJ consists of a sum of cosine functions with phase deviation, modulation frequency, and peak amplitude. The model is given by

$$PJ_T = \sum_{i=0}^{n} a_i \cos\left(\omega_i t + \theta_i\right) \tag{32}$$

where PJ_T denotes the total periodic jitter, n is the number of cosine components, a_i is the amplitude in units of time in each tone, ω_i is the angular frequency of the corresponding modulation, t is the time, and θ_i is the corresponding phase [15].

Sinusoidal jitter in time domain produces a probability distribution function given by (defining time zero as the center of the distribution)

$$J_{PJ_i}(x) = \begin{cases} \dfrac{1}{\pi\sqrt{a_i^2 - x^2}} & |x| \le a_i \\ 0 & otra \end{cases} \tag{33}$$

where $2a$ is the peak-to-peak width of periodic jitter [14]. In Fig. 4b) is shows the histogram for sinusoidal periodic jitter with added random jitter.

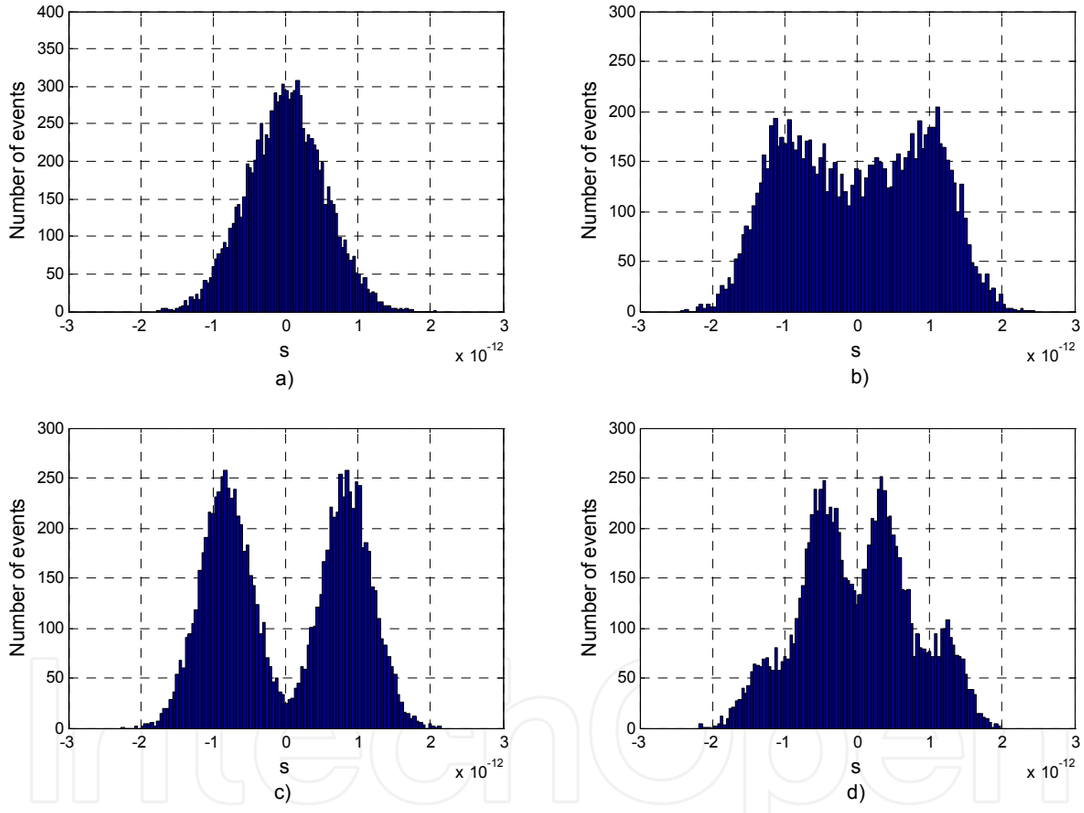


Fig. 4. Histogram for a) Random jitter (RJ), b) Sinusoidal periodic jitter with added random jitter (PJ+RJ), c) duty cycle distortion with added random jitter (DCD+RJ) y d) data dependent jitter with added random jitter (DDJ+RJ).

3.1.3 Duty Cycle Distortion (DCD)

Duty Cycle Distortion is often also called pulse width distortion [14], is deviation in the duty cycle value from the ideal value, this equates to a deviation in bit time between a 1 bit (logic 1) and a 0 bit (logic 0). DCD can have several sources. The most ommon are threshold level offsets and differences in the rising and falling edge characteristics [14].

DCD yields a binomial distribution consisting of two sharp peaks of equal height, unless one separates rising and falling transitions in the measurement. Theoretically those peaks are Dirac delta functions, but in practice random jitter and limited measurement resolution always produce peaks of finite height and finite width. The analytic equation for DCD distribution is the sum of delta functions [14]:

$$J_{DCD}(x) = \frac{\delta(x-a)}{2} + \frac{\delta(x+a)}{2} \tag{34}$$

where $2a$ is the peak-to-peak width of the DCD. In Fig. 4c) is shows the histogram for duty cycle distortion with added random jitter.

3.1.4 Data Dependent Jitter (DDJ)

Data dependent jitter describes timing errors that depend on the preceding sequence of data bits [14]. DDJ is a predominant form of DJ caused by bandwidth limitations of the system or electromagnetic reflections of the signal [16-17]. Since there is always only a limited number of different possible patterns in a data stream of limited length, data dependent timing errors always produce a discrete timing jitter, theoretically DDJ distribution is the sum of two o more delta functions [14]:

$$J_{DDJ}(x) = \sum_{i=1}^{N} \{p_i \delta(x - t_i)\} \tag{35}$$

where $\sum_{i=1}^{N} p_i = 1$ N is number of distinct patterns, p_i is the probability of the particular pattern occurring, and t_i is the timing displacement of the edge following this pattern. In Fig. 4d is shows the histogram for data dependent jitter with added random jitter.

In the simulations, two pulse trains of unitary amplitude are generated. The value of reference frequency was accepted as $f_0 = 1 \times 10^7$ Hz. The hypothetical value of unknown frequency $f_X = 5878815.277629991$ Hz is a result of the accepted value of the period $T_X = 1.701023 \times 10^{-7}$ s, and value of pulse width in both pulse trains is $\tau = 1.0 \times 10^{-9}$ s. The RJ model used is Gaussian distributed with RMS value 0.7 ps. The PJ model is a single-tone sinusoidal with frequency 5 MHz and peak-to-peak value of 10 ps, same peak-to-peak value is assumed in DDJ and DCD jitter models. A component of random jitter is added to the last tree models to generate the jitter models PJ+RJ, DDJ+RJ and DCD+RJ. Such jitter values are selected because of the most typical values for such pulse trains according to [15]. Then the jitter components modeled are applied to the time reference points of each narrow pulse on the two pulse trains. In

3.2 Jitter simulation results

In the first computational experiment is assumed the same magnitude of the jitter in the oscillator under measurement and references oscillator on all models. The experimental results when the two pulse trains started in phase are presented in Table 2, to a simulation time of 0.172 s. In the first row of each table are presented the results obtained without jitter models.

In third column is shown the total number of coincidences obtained with each model for the simulation time and, in the fourth column is shown the number of coincidence where appears the stop event associate to the best approximation in the frequency measurement process (the desired count is represented like 10^r [7]). Program code for computational experiment in Matlab is presented in [22].

Reference Oscillator	Oscillator under test	Total number of coincidences	Coincidence number for best approximation
Without jitter model	Without jitter model	20223	19999
RJ	RJ	20222	19998
	PJ+RJ	20240	20016
	DCD+RJ	20213	19989
	DDJ+RJ	20223	19999
PJ+RJ	RJ	20217	19993
	PJ+RJ	20224	20002
	DCD+RJ	20218	19995
	DDJ+RJ	20218	19994
DCD+RJ	RJ	20226	20002
	PJ+RJ	20218	19995
	DCD+RJ	20218	19994
	DDJ+RJ	20217	19993
DDJ+RJ	RJ	20227	20003
	PJ+RJ	20216	19991
	DCD+RJ	20218	19994
	DDJ+RJ	20223	20000

Table 2. Simulation results with same magnitude of the jitter and pulse trains in phase.

Comparing the results shown in both columns with the values obtained in the simulation that does not include any jitter model, we see that in the presence of jitter the number of coincidence and the number of coincidence pulse associated with the best approach varies depending on model type. The latter implies the position at the time of the coincidence pulse is not fixed since it depends on the jitter component is dominant, in all case $n_0=1701023$ and $n_X=1000000$.

Fig. 5 is presented the relative error obtained by simulation around best coincidence, obtained under condition (30) with $\varepsilon=1\times10^{-12}$ s. In this plot we can see that due to jitter effect some theoretically expected marginal coincidences may disappear or non-theoretically expected may appear. However, this phenomenon can not be observed in non-marginal coincidences, for instance the expected coincidence under condition (30) and an appropriated pulse width τ.

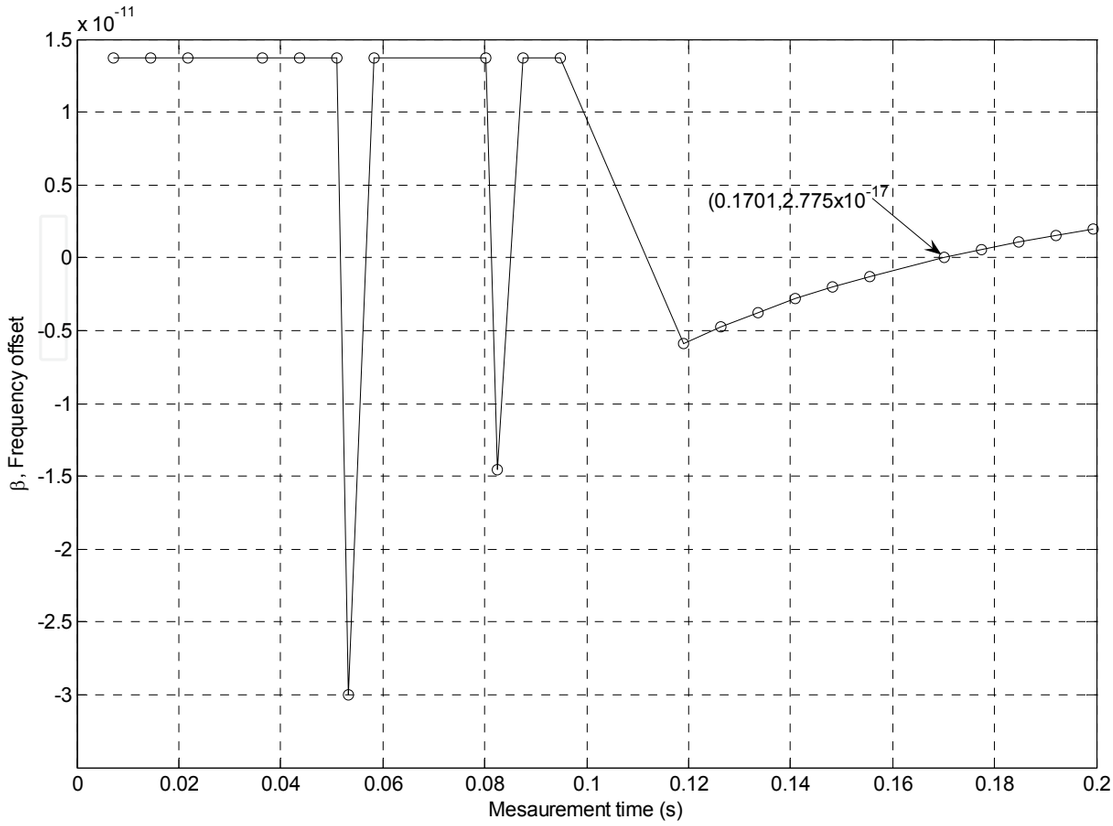


Fig. 5. Jitter effect on frequency relative error for a series of best coincidences (simulation time 0.2.s)

4. Experimental research

For experimental research a prototype of frequency meter was implemented, based on the block diagram shown in Fig 6. This prototype was implement in the FPGA EP3SL150F1152C2N using the development board STRATIX III EP3SL150 and the design software QUARTUS II. In Fig 7. is shown the circuit diagram to the FPGA based frequency measurement prototype used.

For practical frequency measurement, reference frequency was provided by using an Agilent 33250A arbitrary waveform generator and, was set to $f_o = 1 \times 10^7$ Hz. The hypothetical unknown frequency was provided by Tektronix AFG3101 Arbitrary function generator.

In Fig. 8a) is presented arbitrary selection from the experimental data set a period value associate to the hypothetical unknown frequency used in experimental research. As shown in Fig. 8a) the measured unknown frequency was adjusted on the rate of T_x=989.97ns according to in-built equipment frequency counter. Then this unique pulse train frequency was counted by our experimental prototype of frequency meter. The count of pulses from unknown frequency train obtained with the digital counter Q in block diagram of Fig 6 under the condition (30) is show in Fig. 7 b). The measurement time by single

experimentation never exceeds 1 s. It is evident from screenshot Fig. 7 b) that our prototype circuit has a higher resolution than Tektronix AFG3101 in-built frequency counter, but it shows the same rate of frequency. The character of coincidences between indications of experimental prototype and Tektronix AFG3101 generator was the same on all experimental data set. It permits us to make the next important practical conclusion.

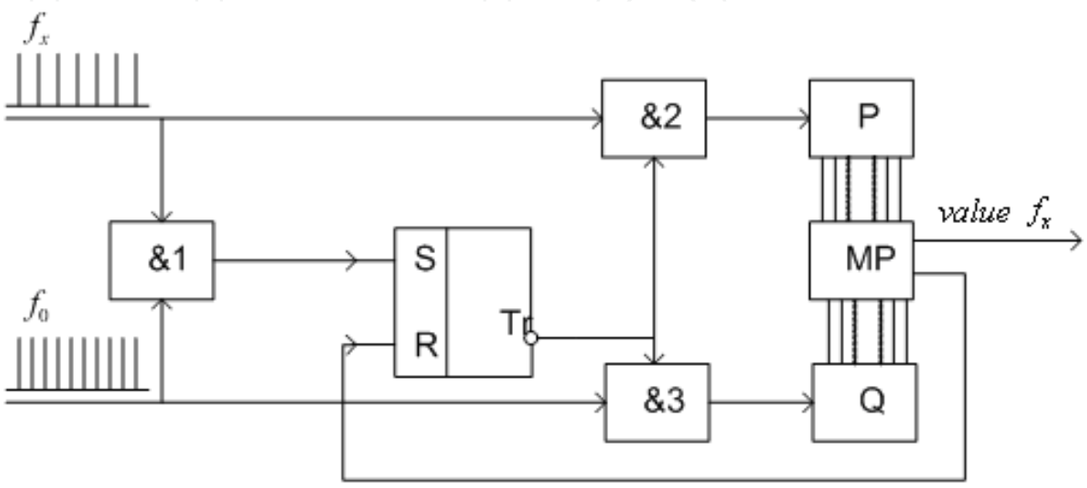


Fig. 6. Frequency meter block diagram.

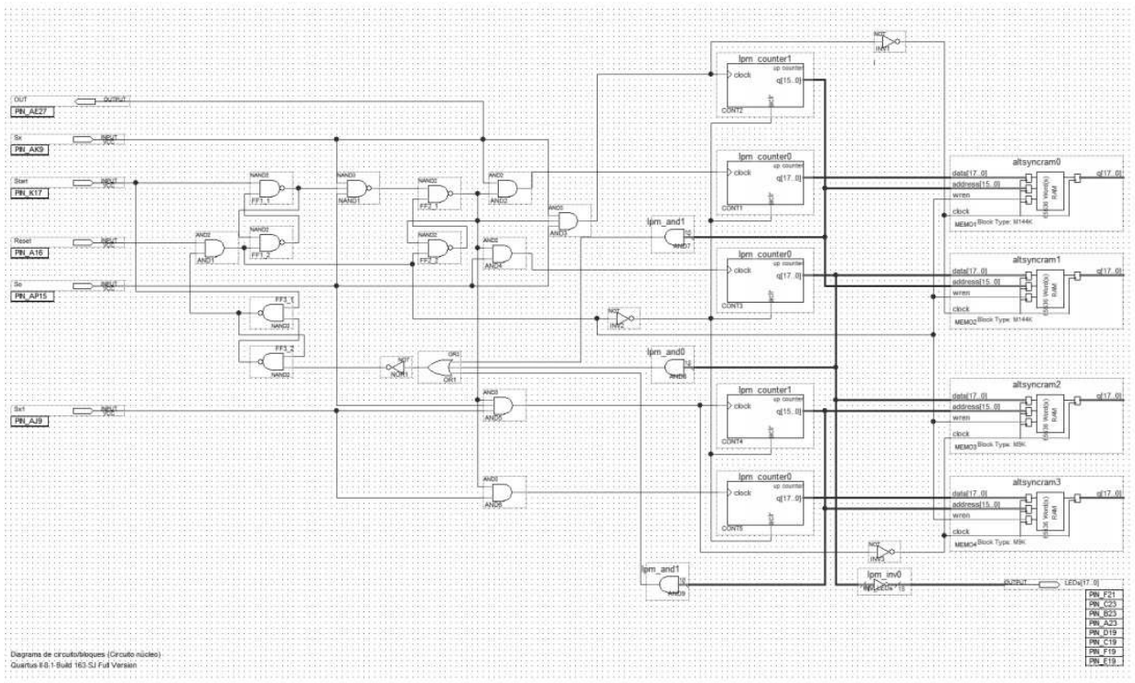
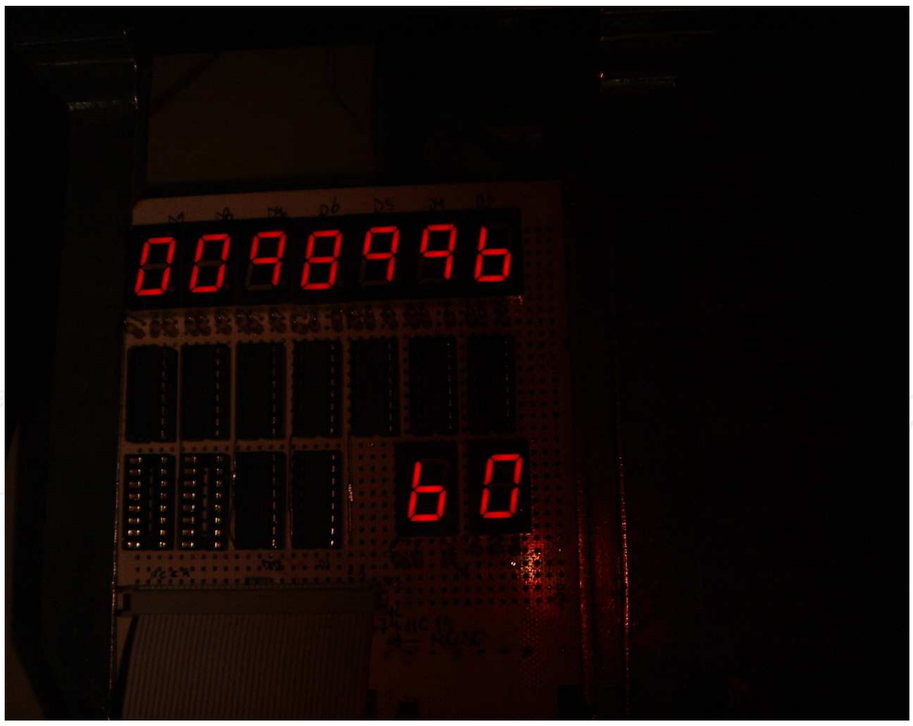


Fig. 7. Circuit diagram for FPGA based frequency meter.



a)



b)

Fig. 8. Sample frequency (formed by arbitrary function generator, a) measurement by prototype circuit (b).

The prototype circuit unfortunately still has multiply sources of noise and uncertainty. But it is a second plan aspect of circuit optimal design in a future work. The main proof of this prototype circuit is the proof of the possibility for a fast frequency measurement without losses of high resolution and rigorous link to actual situation with frequency jitter in a present pulse train.

5. Conclusions

In the offered model for fast frequency measurement, the result is fixed on the equality of intervals n_0T_0 and n_XT_X. Therefore the model is independent to the parameters of coincidence circuits, duration and the shape of coincidence pulses, and the parameters of "zero-crossing" pulses in both sequences.

Due to jitter effect some theoretically expected marginal coincidences may disappear or non-theoretically expected may appear. However, this phenomenon can not be observed in non-marginal coincidences, for instance the expected coincidence under condition (30) and an appropriated pulse width τ.

For measuring systems which can be constructed on the basis of the specified model, systematic and instrumental errors have the same infinitesimal order. Instrumental errors are caused only by the reproducibility of the reference frequency.

For measurements of high values of frequency f_X it is expedient to use higher values of reference frequency in order to have an equivalent reduction of measurement time.

Also it is important to note, that this theoretical method permits to measure unknown frequency value in a case, when unknown frequency exceeds the own value of a standard. For classical methods it is impossible completely.

In future work, there will be an improved version of the experimental prototype to reduce the influence of deterministic errors in measuring and evaluating new frequency estimators based on the Theory of Numbers.

6. References

[1] Stein, S. R. Frequency and Time- Their Measurement and Characterizations. Precision Frequency Control. Vol. 2. Academy Press, New York. 1985. pp 191-416.

[2] Johansson, S. New frequency counting principle improves resolution. Proceedings of the 36 Annual Precise Time and time interval (PTTI) Systems and Application Meeting, 7-9 December 2004, Washington, D.C., ISBN 0-7803-9053-5, 2005 – 628p.

[3] Wei Z. The greatest common factor frequency and its application in the accurate measurement of periodic signals. Proceedings of the 1992 IEEE Frequency Control Symposium, pp. 270-273, 1992.

[4] Fletcher, J. C. Frequency measurement by coincidence detection with standard frequency. U. S. Patent 3, 924,183. 1975.

[5] Tyrsa V.E. Error reduction in conversion of analog quantities to digitized time intervals. Measurement Techniques. Vol 18, No. 3. 1975. pp. 357-360.

[6] Tyrsa V.E., Dunashev V.V. Accuracy of frequency measurement base on the pulses coincidence principle. Measurement Techniques. Vol. 24, No.43. pp. 308-312. 1981.

[7] Hernández-Balbuena D., Sergiyenko O., Tyrsa V., Burtseva, L, Rivas-López M.,. Signal frequency measurement by rational approximations. Elsevier, "Measurement", Volume 42, Issue 1, Pages 136-144, 2009.

[8] Hernández-Balbuena D., Oleg Sergiyenko, Vera Tyrsa, Larisa Burtseva *Frequency measurement method for Mechatronic and Telecommunication applications.* IEEE-IES Proceedings of International Symposium on Industrial Electronics (ISIE-2008), Cambridge, United Kingdom, 30 de junio -2 de julio de 2008, 2008, p.1452-1458, ISBN 978-1-4244-1666-0, ISSN/Library of Congress Number 2007936380.

[9] Hernández-Balbuena D., Oleg Sergiyenko, Vera Tyrsa, Larisa Burtseva. *Method for fast and accurate frequency measurement*. Proceedings of 16th IMEKO TC4 Symposium "Exploring New Frontiers of Instrumentation and Methods for Electrical and Electronic Measurements", Florence, Italy, 20-22 September, 2008. pp. 367-373 [CD-ROM]. ISBN 978-88-903149-3-3.

[10] Murrieta-Rico, Fabián N., O. Yu. Sergiyenko, V. V. Tyrsa, Daniel Hernandez B. W. ernandez. *Frequency domain automotive sensors: resolution improvement by novel principle of rational approximation.* Proceedings of IEEE-ICIT International Conference on Industrial Technology (ICIT'10), 14-17 March, 2010, Viña-del-Mar, Valparaiso, Chile, pp.1293-1298, ISBN 978-1-4244-5697-0/10.

[11] Clarkson V, Perkins J. E., and Mareels I. On the novel application of number theoretic methods to radar detection. *Proc. Internat. Conf. Signal Process. Appl. Tech.*, vol. 1, pp. 1202-1211, Oct 1993.

[12] Clarkson V, Perkins J. E., and Mareels I. Number theoretic solutions to intercept time problems. IEEE Transactions in Information Theory, Vol 42. No. 3. pp 959-971, May 1996.

[13] Tyrsa V., Zenya, A.D. Analysis of errors in frequency comparison by the pulse coincidence method. Measurement Techniques, no. 7, pp. 49-51. 1983.

[14] W. Maichen. Digital timing Measurement. From scope and probes to timing and jitter. FRET 33, Frontier in electronic testing. Springer. Netherland. pp 240. 2006. ISBN 0-387-31418-0.

[15] K. K. Kim et al., Analysis and simulation of jitter sequences for testing serial data channels. IEEE Transactions on Industrial Informatics. Vol 4, No 2. pp 134-143. May 2008.

[16] Buckwalter, et al, Predicting Data-Dependent Jitter. IEEE Transactions on Circuits and Systems-II:Express briefs, Vol. 51, No. 9. 2004. pp 543-457.

[17] B. Analui, et al, Data-Dependent Jitter in Serial Communications. IEEE Transactions on Microwave Theory and Techniques, Vol. 53, No 11, 2005. pp 3388-3397.

[18] ITU-T. Vocabulary of digital transmission and multiplexing, and pulse code modulation (PCM) terms. ITU-T Recommendation G.701. International Telecommunication Union. 1994. p 6.

[19] Sergiyenko O., M. Rivas López, I. Rendón López, V. Tyrsa, L. Burtseva, D. Hernández B. *Possible practical applications of precise optical scanning.* Proceedings of CARS & FOF 07 23rd ISPE International Conference on CAD/CAM Robotics and Factories of the Future, Bogota. Colombia. 16-18 August, 2007, pp. 440-444. ISBN: 978-958-978-597-3.

[20] Sergiyenko O., W. Hernandez, V. V. Tyrsa, Daniel Hernandez B.. *Precise Optical Scanning for multiuse*. Proceedings of IEEE-35th Annual Conference of IEEE

Industrial Electronics (IECON'09), 3-5 November, 2009, Porto, Portugal, pp.3399-3404. ISBN 978-1-4244-4649-0/09.

[21] Rivas-López M., Oleg Sergiyenko, Vera Tyrsa, Wilmar Hernandez Perdomo, Daniel Hernandez B., Luis Devia Cruz, Larisa Burtseva, Juan Iván Nieto Hipólito. *Optoelectronic method for structural health monitoring*. SAGE Publications, International Journal of Structural Health Monitoring, Vol.9, No.2, March, 2010, pp.105-120. Issue Online, September,24, 2009, ISSN 1475-9217 / doi: 10.1177/1475921709340975

[22] Oleg Segiyenko, Daniel Hernandez B., Vera Tyrsa, Patricia Luz Aurora Rosas Méndez, Moisés Rivas Lopez, Filmar Hernandez, Mikhail Podrygalo, Alexander Gurko. Analisis of jitter influence in fase frequency measurements. Elsevier, "Measurement", Volume 46, Issue 7, Agoust 2011, Pages 1209-1328. ISSN: 0263-2241 - doi:10.1016/j.measurement.2008.04.009

IntechOpen



Modern Metrology Concerns

Edited by Dr. Luigi Cocco

ISBN 978-953-51-0584-8
Hard cover, 458 pages
Publisher InTech
Published online 16, May, 2012
Published in print edition May, 2012

"What are the recent developments in the field of Metrology?" International leading experts answer this question providing both state of the art presentation and a road map to the future of measurement science. The book is organized in six sections according to the areas of expertise, namely: Introduction; Length, Distance and Surface; Voltage, Current and Frequency; Optics; Time and Relativity; Biology and Medicine. Theoretical basis and applications are explained in accurate and comprehensive manner, providing a valuable reference to researchers and professionals.

How to reference

In order to correctly reference this scholarly work, feel free to copy and paste the following:

Daniel Hernandez-Balbuena, Oleg Sergiyenko, Patricia L. A. Rosas-Méndez, Vera Tyrsa and Moises Rivas-Lopez (2012). Fast Method for Frequency Measurement by Rational Approximations with Application in Mechatronics, Modern Metrology Concerns, Dr. Luigi Cocco (Ed.), ISBN: 978-953-51-0584-8, InTech, Available from: http://www.intechopen.com/books/modern-metrology-concerns/fast-method-for-frequency-measurement-by-rational-approximations-with-application-in-mecatronics

INTECH
open science | open minds

InTech Europe
University Campus STeP Ri
Slavka Krautzeka 83/A
51000 Rijeka, Croatia
Phone: +385 (51) 770 447
Fax: +385 (51) 686 166
www.intechopen.com

InTech China
Unit 405, Office Block, Hotel Equatorial Shanghai
No.65, Yan An Road (West), Shanghai, 200040, China
中国上海市延安西路65号上海国际贵都大饭店办公楼405单元
Phone: +86-21-62489820
Fax: +86-21-62489821

© 2012 The Author(s). Licensee IntechOpen. This is an open access article distributed under the terms of the Creative Commons Attribution 3.0 License, which permits unrestricted use, distribution, and reproduction in any medium, provided the original work is properly cited.

IntechOpen

IntechOpen